Microviscosity in Poly(ethylene oxide)-Polypropylene Oxide-Poly(ethylene oxide) Block Copolymers Probed by Fluorescence Depolarization Kinetics

SANGMIN JEON[1], STEVE GRANICK[1], KWAN-WOOK KWON[2], KOOKHEON CHAR[2]

[1] Department of Materials Science and Engineering, College of Engineering, University of Illinois, Urabana-Champaign, 1304 West Green Street, Urbana, Illinois 61801

[2] School of Chemical Engineering, Seoul National University, Seoul 151-744, Korea

Received 24 January 2002; revised 9 September 2002; accepted 10 September 2002

ABSTRACT: Triblock copolymers [poly(ethylene oxide) (PEO) and polypropylene oxide (PPO)], Pluronic F127 with 100 PEO blocks on each end, and 65 blocks of PPO in the center were examined in aqueous solution. The "sol" and "gel" phase diagram was determined as a function of concentration and temperature. For further study, the concentration was fixed at 20 wt %, and the temperature dependence of the dynamic viscosity differed from the temperature dependence of fluorescence emission spectra and the microviscosity probed by the fluorescence depolarization kinetics of rhodamine 123 dye, which was dissolved in the continuous hydrophilic phase. The depolarization measurements used single-photon counting after two-photon excitation with a Ti-sapphire femtosecond laser. Although the viscoelastic modulus increased by an order of magnitude when the sol-to-gel transition was crossed, the microviscosity of the hydrophilic continuous medium showed only minor changes. At different temperatures the fluorescence lifetime was the same with a single-exponential time constant, but the fluorescence depolarization displayed a double-exponential decay. After comparison with fluorescence depolarization of the dye in PPO melt and PEO whose molecular weight and aqueous concentrations were varied, the relative proportions of faster and slower components of the fluorescence depolarization were tentatively attributed to varying ratios of the dye in free solution and associated with micelles. © 2002 Wiley Periodicals, Inc. J Polym Sci Part B: Polym Phys 40: 2883–2888, 2002

INTRODUCTION

Triblock copolymers of poly(ethylene oxide) (PEO) and polypropylene oxide (PPO) are soluble in water but present an interesting sol-to-gel phase transition over a wide range of concentrations in the vicinity of room temperature. For this reason, micellar solutions of PEO-PPO-PEO block copolymers have been extensively researched because of their wide applications in areas from detergents to potential drug-delivery agents.[1–10]

At the temperatures of interest, the PEO block is more soluble in water than the PPO block, and aqueous solutions show lower critical solution temperature (LCST) behavior. When the temperature exceeds this PPO/water LCST temperature and the concentration exceeds the critical micelle concentration, micelles form whose core is PPO and whose corona is PEO. As the temperature is further raised, the abundance of unimers decreases, whereas the number of micelles in-

Correspondence to: S. Granick (E-mail: granick@mrl.uiuc.edu)

Journal of Polymer Science: Part B: Polymer Physics, Vol. 40, 2883–2888 (2002)

creases. Once the volume fraction of micelles reaches the critical volume fraction of closed cubic packing (i.e., 0.523), it forms a gel. For the same triblock copolymer examined here, Prud'homme et al.[4] previously measured the size of the PPO core and the aggregation number of micelles with small-angle neutron scattering. They showed that the micellar core radius (~4.4 nm) and the aggregation number of the micelles (~50) were independent of micellar concentration and temperature.[4] However, Wanka et al.[5] reported that if the polymer concentration is sufficiently low (too low for gelation and lower than in this study), the aggregation number of F127 increases continuously from 1 to 106 with increasing temperature.

When the temperature is sufficiently high, the diminishing solubility of the PEO block in water causes the size of the PEO blocks to shrink, and consequently the hydrodynamic size of the micelle decreases. Studies show that the viscosity of this reversible gel remarkably exceeds that of a sol phase owing to jamming interactions because the micelle–micelle interaction is repulsive.[11]

In this article, we are interested in contrasting the macroscopic viscosity of these microstructured systems with local environments as reflected in the mobility of tracer molecules embedded within the continuous phase. Concerning the question of mobility within the cores of the PEO-PPO-PEO micelles, much is known already from the work of Nivaggioli and coworkers[12–16] who used a combination of fluorescence spectroscopy and small-angle neutron scattering. Instead, we address the microenvironment in the PEO-rich continuous phase. From related work concerning tracer mobility within metal alkoxide gels, the mobility of small tracers inside those systems is little affected by gelation.[17–19] The quantitative characterization of the changes of mobility with temperature is the main contribution of this study.

EXPERIMENTAL

The fluorescence measurements were conducted at the University of Illinois. Other measurements including the phase diagram were conducted at the Seoul National University.

Time-Resolved Fluorescence Anisotropy

Time-resolved fluorescence anisotropy is a method by which rotational relaxation times are characterized on the nanosecond timescale. In this way, the rotational motions of a fluorescent molecule are used to probe the local microenvironment in which they reside.

Two-photon excitation of the fluorescent probe molecules was induced with a femtosecond Ti: sapphire laser (Mai Tai, Spectra-Physics) whose full width at half-maximum pulse was 100 fs. The repetition rate was 80 MHz, and the wavelength was 800 nm. The experiments were performed within a homemade microscope designed to combine this measurement with the surface forces apparatus. However, a perfusion chamber (Sigma) with 1.3 mm total thickness was used in these initial experiments to simplify the surface geometry.

In the design that we used, the vertically polarized laser beam was first split into two beams, and one of them was introduced into an objective lens [Mitutoyo, numerical aperture (N.A.): 0.55] and focused onto the sample. The other beam was used as a trigger signal for the single-photon counting system (Becker & Hickl GmbH, Berlin, Germany). The emitted fluorescence was collected by the same objective lens and focused again by a tube lens into photo-multiplier-tube (PMT) detectors. A fast PMT (Hamamatsu, R5600) and a photodiode were used to detect the fluorescence and the trigger signal, respectively. The PMT signal was input to the time-to-amplitude converter as a start signal followed by a constant fractional discriminator (Becker & Hickl GmbH, TCSPC730). In this setup, the total instrument response function was around 150 ps. The instrument and measurement protocol have been described in detail elsewhere.[20]

To measure the fluorescence emission spectra, a commercial instrument (QuantaMaster, Photon Technology International) was used without modification.

Determination of the Gel Point by Tube Inversion

Vials with a diameter of 13 mm were sealed with Teflon tape and placed in a water bath to control temperature with an accuracy of ± 0.01 °C. To ensure equilibrium, at least 10 min of temperature equilibration were allowed at each temperature. Measurements were performed at 0.5 °C increments from 1 to 90 °C. Change from a mobile state to an immobile one was determined by inverting the vial. Gels were defined as immobility of the solution (i.e., no movement of the liquid meniscus in the vial for more than 5 min), whereas sols were defined as those that readily

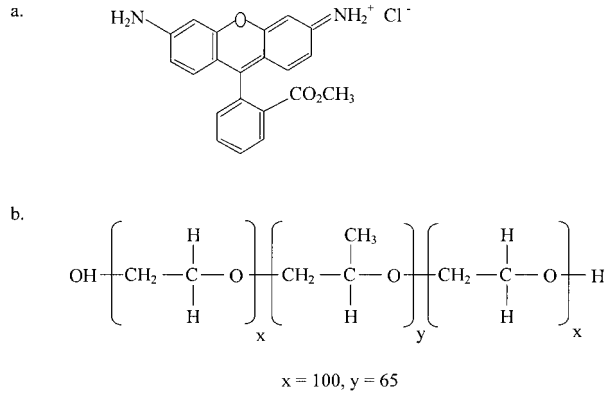

Figure 1. Chemical structure of the hydrophilic dye, rhodamine 123, and the PEO-PPO-PEO triblock copolymer.

flowed to the bottom of a tube within 5 min after inversion.

Rheology

A Rheometer RMS-800 (Rheometrics Scientific, Inc.) in a coni-cylinder geometry (cup diameter: 52 mm; bob diameter: 50 mm; bob length: 20 mm; and bottom gap: 0.2 mm) was used to measure the dynamic viscoelastic elastic modulus G' and viscous modulus G'' of the polymer solutions as a function of temperature. Temperature scans at the fixed radian frequency ω = 0.5 rad/s were carried out at a heating rate of 1 °C min^{-1} from 4 to 40 °C. Strain was fixed at 2.7%, which was small enough to ensure linear viscoelasticity. The dynamic viscosity, η^*, was calculated as $\eta^* \equiv [G'^2(\omega) + G''^2(\omega)]^{1/2}/\omega$.

Materials

The chemical structures of the PEO-PPO-PEO triblock copolymer used in this study and of the rhodamine 123 dye (Aldrich) are shown in Figure 1. In most experiments, the triblock copolymers were purchased from BASF (Pluronic F127 Prill) and used without further purification. As reported by the manufacturer, it consists of 100 PEO segments on each end and 65 repeat units of PPO at the center. The number-average molecular weight (M_n) was ≈12,600; the polydispersity is not known. The final polymer concentration was prepared to 20 wt %, and rhodamine 123 was dissolved in the continuous water phase with a concentration of 1.8 μM. To avoid gelation, it was stored in a refrigerator before use.

For control experiments, a PPO homopolymer (M_n = 2000) and a PEO homopolymer (M_n = 400) were purchased from Aldrich; the molecular weights of these samples were selected so that they were all liquids at room temperature. In addition, monodisperse anionically synthesized PEO (M_n = 21,000) was purchased from Tosoh (Japan).

To disperse the fluorescent dye in the melts of PPO and PEO-PPO-PEO, polymers with the dye were initially dissolved in spectroscopic grade methanol (Mellanckrodt), stirred vigorously with a vortex mixer, and finally the methanol was evaporated at 80 °C under low pressure for 8 h. Complete drying was confirmed by measuring the total mass before and after the evaporation.

RESULTS AND DISCUSSION

Phase Diagram

Figure 2 illustrates the measured phase diagram of the triblock copolymer in deionized water at different concentrations and temperatures. Although only a sol phase was observed when the concentration was lower than 16 wt %, above that concentration we found three of the following regimes as the temperature was varied: sol at low temperature, gel at intermediate temperatures, and sol at even higher temperatures (for the reasons discussed in the introduction). At the concentration of 20.0 wt %, at which fluorescence

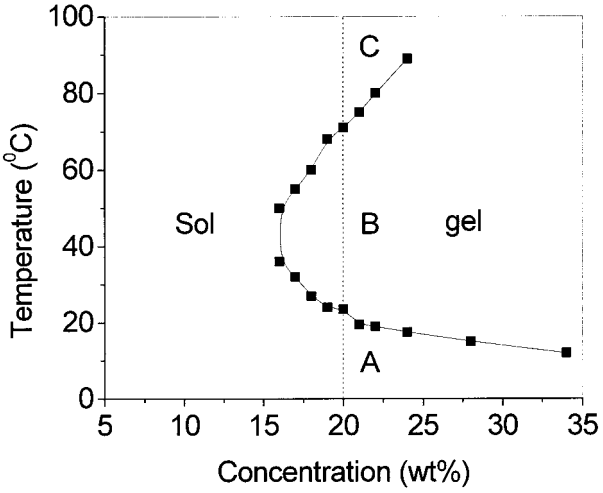

Figure 2. Phase diagram of the PEO-PPO-PEO block copolymer in deionized water as measured by the tube-inversion method. The dashed vertical line indicates the polymer concentration at which fluorescence experiments were conducted.

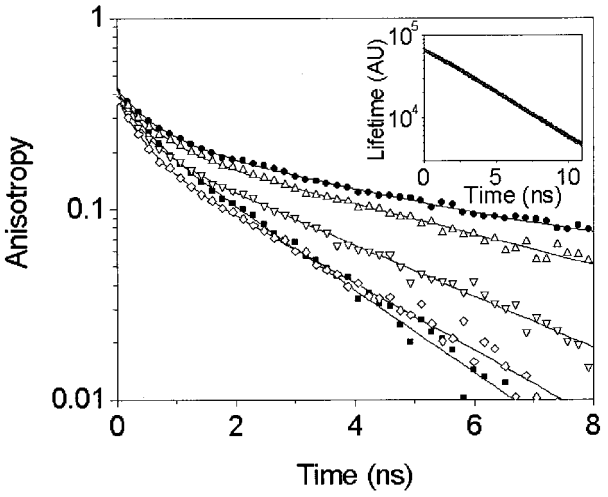

Figure 3. Fluorescence anisotropy of rhodamine123 plotted against elapsed time on the nanosecond timescale at various temperatures: 15 °C (■), 20 °C (●), 25 °C (△), 30 °C (▽), and 35 °C (◇). Filled symbols and open symbols represent the sol–gel phase. All data are averaged with adjacent two points for clarity. The curves were fitted with second-order exponential functions summarized in Table 1. In the inset, the fluorescence lifetime is plotted semilogarithmically against elapsed time, showing the lack of temperature dependence.

measurements to determine the microstructural mobility were made, the sol-to-gel transition occurred at 23.5 °C. Song et al.[21] measured the critical micelle temperature and micellar volume fraction of the same copolymer and concentration with dielectric relaxation spectroscopy. Micelles start to appear at 12 °C. The micellar volume fraction increases up to 40 °C and then slowly decreases. Because the temperature here varied from 15 to 35 °C, over the temperature range that we covered, the volume fraction of micelles increased as the temperature increased.

Rotational Relaxation Times and Fluorescence Lifetimes in the Hydrophilic Microenvironment

Figure 3 portrays the effect of temperature on the fluorescence depolarization of the fluorescent probe molecules; anisotropy is plotted semilogarithmically against decay time. The anisotropy, r, is defined as

$$r \equiv (I_{VV} - G\, I_{VH})/(I_{VV} + 2\, G\, I_{VH})$$

where G is the compensating factor for the two-photon detectors described elsewhere,[22] I is the intensity, the first subscript refers to the laser polarization, and the second subscript refers to the direction of fluorescence polarization. For example, I_{VH} is the intensity of horizontally polarized fluorescence excited by a vertically polarized laser beam. A homebuilt thermoelectric stage was used for the temperature control (±0.1 °C).

The anisotropy decays were well fitted with double-exponential functions with PicoQuant FluoFit software (PicoQuant GmbH), and their relative amplitudes and time constants are listed in Table 1. Contrary to the large increase in the viscosity of a bulk solution when the gel point is reached, no abrupt change of the rotational correlation times was observed. Instead, the faster time constant monotonically decreased over the entire span of temperature, whereas the longer time constant went through a maximum near the gel point temperature. The physical interpretation, which is based on the fluorescence experiments, indicates that the local microenvironment did not change abruptly near the bulk transition.

The inset of Figure 3 illustrates the fluorescence lifetime decay of the dye; the fluorescence intensity is plotted against lag time. We observed the single-exponential decay time constant of 4.3 ns regardless of temperature. This implies that the fluorescent probes experienced the same microenvironment. Because the rhodamine 123 dye had a positive charge and the PEO repeat unit had slight electronegativity, some preferential association of the dye with PEO can be expected. To test more directly to what extent the fluorescent probes interact with PEO, the fluorescence emission spectra were examined.

Figure 4 displays the fluorescence emission spectra at room temperature in deionized water, in PPO, and in PEO solutions of different sorts. The maximum emission wavelengths from deionized water, 10 wt % PEO (M_n = 400), 30 wt % PEO (M_n = 400), PPO melt (M_n = 2000), and 20

Table 1. Fitting Parameters for Anisotropy Decay of Rhodamine 123 in the Same PEO-PPO-PEO Solutions at Different Temperatures

T(°C)	A_1(%)	τ_1(ns)	A_2(%)	τ_2(ns)
15	46.4	0.57	53.6	2.55
20	44.3	0.52	55.7	4.28
25	43.9	0.52	56.1	4.39
30	44.4	0.43	55.6	3.29
35	48.5	0.39	51.5	2.59

The parameters A_1 and A_2 denote the relative amplitudes of the respective time constants, τ_1 and τ_2.

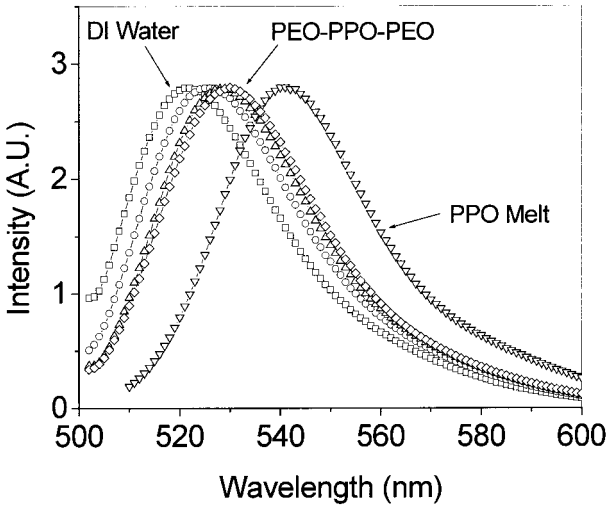

Figure 4. Fluorescence emission of rhodamine 123 was measured as a function of wavelength when the dye was dissolved in various homogeneous environments: deionized water (□); PEO solutions (M_n = 400) of concentration 10% PEO (O) and 30% PEO (△); undiluted PPO melt with M_n = 2000 (▽); and 20% PEO-PPO-PEO triblock copolymer with M_n = 2000 (◇).

wt % PEO-PPO-PEO solutions are λ_{max} = 521, 526, 529, 541, and 530 nm, respectively. Here, emission of the dye in the PPO melt was used to represent the environment of the micellar core; observing its different λ_{max} from that of the probe dissolved in triblock copolymers confirms that it resides in the continuous matrix rather than in the micellar core. Detailed examination of the emission curves in Figure 4 shows that the emission spectrum from PEO-PPO-PEO triblock copolymers was similar to that from 30 wt % of PEO aqueous solution. This implies that the probes resided in the hydrophilic matrix but left open the question of possible aggregation with PEO.

Table 2 evaluates the lifetimes and anisotropy decay characteristics in these same media. Although the fluorescence lifetime in water and all of the PEO solutions was 4.3 ns regardless of the concentration of PEO or its molecular weight, the lifetime in the PPO melt was significantly less (3.5 ns). This again confirms that the probes were located in hydrophilic regions rather than the PPO micellar core. When rhodamine 123 was dissolved in deionized water, its fluorescence anisotropy displayed a single-exponential decay, and its rotational correlation time constant was 0.21 ns without deconvolution of the instrument-response function. However, this decay time constant increased with increasing concentration of the lower-molecular-weight PEO.

In addition, the environment of a PEO sample of higher molecular weight resulted in a double-exponential anisotropic decay curve. When one of the time constants was fixed at the same value measured directly in deionized water (0.21 ns), the decay curve was well fitted, suggesting that the weight of this time constant reflects the relative proportion of dyes in free (unassociated) solution. By inference, the other decay time is associated with the population of the dye associating with the PEO matrix.

In the case of the matrix of the low-molecular-weight PEO matrix, all the fluorescent probes appear to associate with the matrix, but this was not so for the matrix of higher-molecular-weight PEO. Similarly, the anisotropy decay of the dye in the PEO-PPO-PEO triblock matrix was more complex than could be fitted with a single-exponential function. Also, it could not be fitted with one time constant fixed at the value measured in deionized water (0.21 ns), which implies that the abundance of dyes free in solution was low. Instead, the anisotropy decay at 20 °C could be well fitted with two slower time constants, 0.51 and 4.2 ns. We speculate that the shorter and longer time constants can be assigned to the aggregation with PEO in unimers and micelles, respectively. Godward et al.[23] measured both fast and slow relaxation of protons in the PEO block and PPO

Table 2. At the Constant Temperature of 20.0 °C, Fluorescence Lifetimes and Fitting Parameters for Fluorescence Anisotropy Decay Times are Compared for Rhodamine 123 in Various Aqueous Environments

Medium	Lifetime (ns)	A_1(%)	τ_1(ns)	A_2(%)	τ_2(ns)
Deionized water	4.35 ± 0.014	100	0.21 ± 0.003	–	–
PEO400 10%	4.35 ± 0.023	100	0.33 ± 0.005	0	–
PEO400 30%	4.34 ± 0.012	100	0.72 ± 0.004	0	–
PEO21K 10%	4.35 ± 0.014	63	0.21 (Fixed)	37	0.95 ± 0.048
PPO2K Melt	3.51 ± 0.009	100	16.1 ± 1.7	0	–
PEO-PPO-PEO 20%	4.30 ± 0.005	56	4.2 ± 0.11	44	0.51 ± 0.011

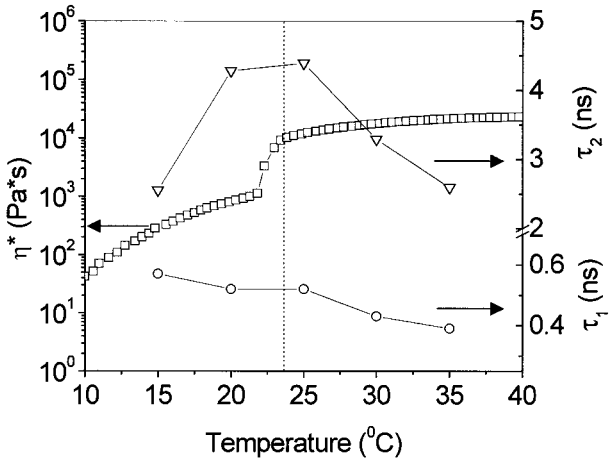

Figure 5. Complex dynamic viscosity determined from the dynamic mechanical viscoelastic modulus at 0.5 rad/s plotted on a log scale (left ordinate axis) against temperature and compared with the rotational correlation time constants, τ_1 and τ_2, of the probe in the continuous phase (right coordinate axis). Heating rate for bulk viscosity measurement was 1°/min. The dashed vertical line shows the temperature of the sol-to-gel transition.

block directly on the basis of an NMR experiment, and they assigned the fast and slow correlation time constants to the segmental motion and the larger-scale motion, respectively.

The microviscosity of reversible polymer gel could be calculated from τ_1 in Table 1 with a suitable model. Because there is no available simple model for the complexation of the probe with the triblock copolymer, the rotational correlation time constants are compared with bulk viscosity in Figure 5. Although the bulk dynamic viscosity increased by nearly an order of magnitude at the gel point and continued to increase with increasing temperature, the faster rotational time constant decreased monotonically. We attribute this partly to the loss of unimers to micelles and partly to more rapid motion at the higher temperature.

Compared with τ_1 that is related to the microviscosity of the continuous phase, τ_2 can be related to the structure of the micelles because the origin of τ_2 is the interaction between the probe and PEO chains in the micelles. The volume fraction of micelles increases with increasing temperature up to 40 °C,4 impeding the free movement of PEO chains. However, PEO chains shrink as the solvent quality decreases approaching the LCST. This balanced tendency may explain that the slower rotational correlation time, τ_2, was slowest at temperatures close to the sol-to-gel transition and faster on both sides of it.

At the University of Illinois, this work was based on work supported by the U.S. Department of Energy, Division of Materials Science (under award DEFG02-91ER45439), through the Frederick Seitz Materials Research Laboratory at the University of Illinois at Urbana-Champaign. K.-W. Kwon and K. Char at the Seoul National University acknowledge the support from the National Research Laboratory Fund of the Ministry of Science and Technology (MOST).

REFERENCES AND NOTES

1. Alexandridis, P.; Nivaggioli, T.; Hatton, T. Langmuir 1995, 11, 1468.
2. Kositz, M.; Bohne, C.; Alexandridid, P.; Hatton, T.; Holzwarth, J. Macromolecules 1999, 32, 5539.
3. Mortensen, K.; Brown, W.; Norde, B. Phys Rev Lett 1992, 68, 2340.
4. Prud'homme, R.; Wu, G.; Schneider, D. Langmuir 1996, 12, 4651.
5. Wanka, G.; Hoffmann, H.; Ulbricht, W. Macromolecules 1994, 27, 4145.
6. Nystrom, B.; Kjoniksen, A. Langmuir 1997, 13, 4520.
7. Glatter, O.; Scherf, G.; Brown, W. Macromolecules 1994, 27, 6046.
8. Malmsten, M.; Lindman, B. Macromolecules 1992, 25, 5440.
9. Nakashima, K.; Takeuchi, K. Appl Spectrosc 2001, 55, 1237.
10. Hecht, E.; Mortensen, K.; Gradzielski, M.; Hoffman, E. J Phys Chem 1995, 99, 4866.
11. Mortensen, K.; Pedersen, J. Macromolecules 1993, 26, 805.
12. Nivaggioli, T.; Tsao, B.; Alexandridis, P.; Hatton, T. Langmuir 1995, 11, 119.
13. Nivaggioli, T.; Alexandridis, P.; Hatton, T. Langmuir 1995, 11, 730.
14. Alexandridis, P.; Athanassiou, V.; Hatton, T. Langmuir 1995, 11, 2442.
15. Goldmints, I.; Gottberg, F.; Smith, K.; Hatton, T. Langmuir 1997, 13, 3659.
16. Goldmints, I.; Holzwarth, J.; Smith, K.; Hatton, T. Langmuir 1997, 13, 6130.
17. Ferrer, M.; Monte, F.; Levy, D. J Phys Chem B 2001, 105, 11076.
18. Biermann, U.; Mikosch, W.; Dorfmuller, T.; Eimer, W. J Phys Chem 1996, 100, 1705.
19. Marchi, M.; Bilmes, S.; Negri, M. Langmuir 1997, 13, 3665.
20. Jeon, S.; Bae, S.; Granick, S. Macromolecules 2001, 34, 8401.
21. Song, M.; Lee, D.; Ahn, J.; Kim, D.; Kimi, S. Polym Bull 2000, 43, 497.
22. Lakowicz, J. Principles of Fluorescence Spectroscopy, 2nd ed.; Plenum: New York, 1999.
23. Godward, J.; Heatley, F.; Booth, C. J Chem Soc Faraday Trans 1995, 91(10), 1491.